# Impedance Matrix Compression Using Adaptively Constructed Basis Functions

Zachi Baharav and Yehuda Leviatan, *Senior Member, IEEE*

*Abstract*— **Wavelet expansions have been employed recently in numerical solutions of commonly used frequency-domain integral equations. In this paper, we propose a novel method for integrating wavelet-based transforms into existing numerical solvers. The newly proposed method differs from the presently used ones in two ways. First, the transformation is affected by means of a digital filtering approach. This approach renders the transform algorithm adaptive and facilitates the derivation of a basis which best suits the problem at hand. Second, the conventional thresholding procedure applied to the impedance matrix is substituted for by a compression process in which only the significant terms in the expansion of the (yet unknown) current are retained and subsequently derived. Numerical results for a few TM scattering problems are included to demonstrate the advantages of the proposed method over the presently used ones.**

to perform the transform adaptively. We also use a new method in which the conventional thresholding procedure applied to the impedance matrix is substituted for by a compression process. In the compression, process only the significant terms in the expansion of the (yet unknown) current are retained and subsequently derived by solving a reduced-size matrix equation. This implies that we no longer view the impedance matrix and the excitation vector as arrays of numbers, but rather exploit the understanding of the physics behind these numbers.

The organization of the paper is as follows. In the following section, we discuss a method to transform a conventional impedance matrix, obtained by using regular pulse-basis func-

To transform the pulse basis functions into wavelet basis functions, one introduces a transformation matrix $[T]$ which is assumed to be real and orthogonal. The rows of $[T]$ describe the new wavelet basis functions in terms of the pulses. The basis transformation is effected by

$$\vec{A} = [T]\vec{I} \tag{3}$$

where the elements of $\vec{A}$ are the coefficients of a new series-expansion for $J_z$. In this new series expansion, the basis functions are piecewise constant wavelet functions.

Subsequently, a similar procedure is applied to the rows of the impedance matrix. This transformation is effected by multiplying the impedance matrix on the right by $[\tilde{T}]$, the transpose of $[T]$. We have

$$[Z_A] = [Z][\tilde{T}]. \tag{4}$$

Substituting (3) and (4) into the system (2), and using the fact that $[T]$ is orthogonal, leads to the matrix equation

$$[Z_A]\vec{A} = \vec{V}. \tag{5}$$

It is important to note that as far as the result for the unknown current $J_z$ is concerned, the solution will be the same regardless of whether one uses (2) or (5). Information is neither gained nor lost in this process of basis transformation.

When a Galerkin method is used, it is customary to apply the same transformation used for the basis functions to the testing procedure. Along these lines, we obtain

$$\vec{B} = [T]\vec{V} \tag{6}$$

where $\vec{B}$ is the new excitation vector. Then, we define a matrix $[\mathcal{Z}]$ as the column transformation of $[Z_A]$

$$[\mathcal{Z}] = [T][Z_A] = [T][Z][\tilde{T}] \tag{7}$$

and arrive at the matrix equation

$$[\mathcal{Z}]\vec{A} = \vec{B}. \tag{8}$$

This matrix equation is also equivalent, in terms of $J_z$, to the two previous matrix equations given by (2) and (5). However, in (8), both the sources and testing functions are given in terms of the new basis functions.

A similar idea of basis transformation has been explored in [4], where the transformation has been used to obtain a windowed Fourier transform of the signal. Other related works include those of Canning (Impedance Matrix Localization) [5], [6] and Wagner *et al.* [7].

## III. Discrete Signal Wavelet Transform: Matrices and Filters

In this section, instead of using a transformation matrix, the basis transformation from pulses to wavelets is affected by using a cascade of filters [8]. An extensive literature on the equivalence between these two ways of computing the wavelet transform can be found in [9] and [10]. Here, we only show this equivalence by means of an example. In this example, the Haar wavelets are used and we apply the transform to a four-element signal.

Fig. 1(a), illustrates how the basic signal $\vec{I}$ is transformed by $[T]$ into the new vector $\vec{A}$. Note that the rows of $[T]$ describe the new basis functions. The fact that the new basis is orthonormal can be verified by computing $[T][\tilde{T}]$. In Fig. 1(b), we write explicitly the series expansion in term of the new basis functions. Fig. 1(c)–(d) are related to the computation of the transform by the use of a hierarchical filter structure. Fig. 1(c) illustrates this hierarchical structure. The input signal, described as a discrete sequence, undergoes filtering and down-sampling to produce two output sequences. One sequence contains the high-band (rapidly varying or detailed) parts of the signal while the other contains the low-band (slowly varying or smooth) parts of the signal. The filters denoted by $G$ and $H$ are low-pass and high-pass filters, respectively. They are determined by the wavelet transform one intends to achieve. In the case of the Haar wavelets, their impulse responses are given by $g = \frac{1}{\sqrt{2}}[1, 1]$ and $h = \frac{1}{\sqrt{2}}[-1, 1]$, respectively. The down-sampling operation implies taking every other sample at the output of the filters. For the wavelet decomposition, this process of band splitting is applied recursively to the low-band portion of the signal. The resulting hierarchical structure is described as a tree, as shown in Fig. 1(d), where each node and its associated two branches represent the basic building block. The reconstruction process is similar in both cases, that is, by multiplying with the transpose matrix, or by reversing the graph.

Note that in the implementation of the transform, the fact that the input signal is of finite extent should be accounted for and indeed several approaches to this problem have been suggested [10]. Here, we have resorted to the use of a cyclic convolution while taking only the even-indexed samples at the output of the down sampler.

## IV. Wave Packets

While the two ways of accomplishing the basis transformation (either by matrix multiplication or by digital filters) are mathematically equivalent, the digital filter approach allows the use of many ideas from the signal-processing discipline. These ideas often provide better insight into the choice of basis transformation, but one should recall that any kind of transformation which can be achieved by digital filters can also be attained, though usually with more effort, by a matrix multiplication.

First, the digital filters suggest a fast way for performing the transform [11]. This is owing to the hierarchical structure previously described. Moreover, the tree-structure dictated by the wavelets can be altered and this can very well be done adaptively, as will be discussed later on [12], [13]. In this section, we discuss only two tree-structures (which may be viewed as two extreme cases): wavelet-transform and windowed Fourier transform trees. The windowed Fourier

$$\vec{A} = [T]\vec{I} = \frac{1}{2}\begin{bmatrix} -\sqrt{2} & \sqrt{2} & 0 & 0 \\ 0 & 0 & -\sqrt{2} & \sqrt{2} \\ -1 & -1 & 1 & 1 \\ 1 & 1 & 1 & 1 \end{bmatrix}\begin{bmatrix} I_1 \\ I_2 \\ I_3 \\ I_4 \end{bmatrix}$$

(a)

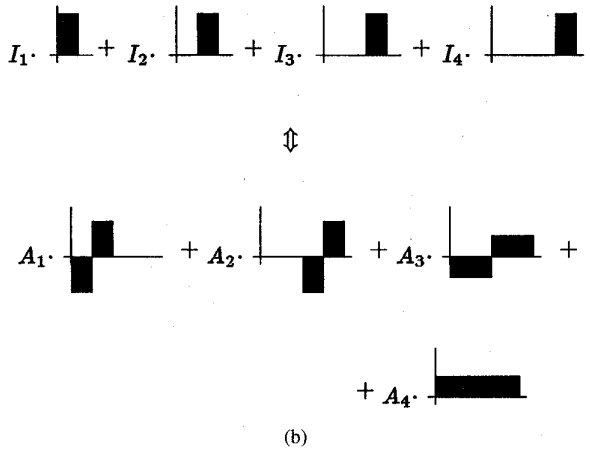


(b)

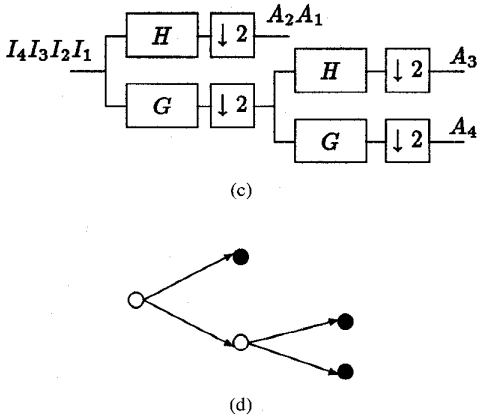


(c)



(d)

Fig. 1. Wavelet transform in different representations. (a) Matrix representation. (b) Pictorial description of the series expansion in terms of the different basis functions. (c) Filter representation. (d) Tree representation.

transform tree, as well as its associated transformation matrix, are shown in Fig. 2.

In the wavelet transform tree structure, shown in Fig. 1(d), only the slowly varying part of the signal is decomposed at each stage. In contrast, in the windowed Fourier transform tree structure, shown in Fig. 2(c), *both* the slowly and rapidly varying components of the signal are decomposed at each stage. We will not examine in what way the partitions of the combined space of location and spatial variation to which these two methods lead are different. We will only point out the fact that windowed Fourier transform basis functions are all of the same length [see Fig. 2(b)]. This is in contrast to the wavelet basis functions, in which the rapidly varying basis functions are of shorter length (see Fig. 1(b), lower part). This suggests that the windowed Fourier transform basis functions, unlike the wavelet basis functions are, in essence, global basis functions.

$$[T] = \frac{1}{2}\begin{bmatrix} 1 & -1 & -1 & 1 \\ -1 & 1 & -1 & 1 \\ -1 & -1 & 1 & 1 \\ 1 & 1 & 1 & 1 \end{bmatrix}$$

(a)

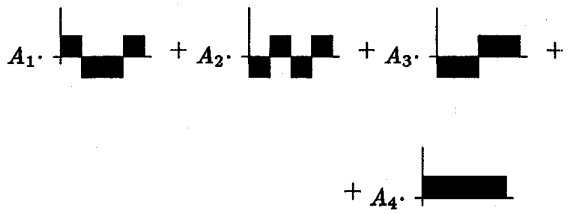


(b)

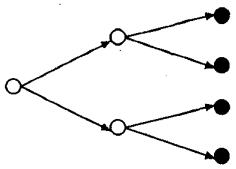

(c)

Fig. 2. An example of a wave-packet described by means of (a) a transformation matrix, (b) a sum of series of basis functions, and (c) a tree-structure.

## V. Adaptive Construction of Basis Functions

As has been pointed out, there are many possible tree structures and, correspondingly, many transformations, each producing a different set of basis functions. Our objective is to determine a basis which best suits the problem at hand. The quality criterion that will serve as a measure of what is best for our purposes is the extent to which the boundary condition is satisfied for a given level of compression of the transformed matrix equation. Thus, we search for a basis that yields minimum boundary condition error for a given matrix size or, equivalently, one that allows maximum reduction in size for a prescribed boundary condition error.

The new approach of basis selection to best address the problem at hand is effected in two steps. In the first step, we construct a vector $\vec{V}$ which is a modified version of the vector $\vec{V}$. This modified version takes into account the shadow region cast by the scatterer, as predicted by geometrical optics. Specifically, the elements of the vector $\vec{V}$ that correspond to testing points in the lit region remain unchanged while those that correspond to testing points in the shadow region are gradually set to zero using a cosine windowing which allows for a smooth transition between the lit and shadow regions. In the second step, a tree is constructed in the following adaptive manner. Starting from the finest resolution level of the vector $\vec{V}$ at the input node, a decision whether to go on decomposing any given node, and stepping down to a coarser resolution level, is made based on a nodal minimum coefficient-spread criterion. The decision concerning further decomposition of a given node is made independently of any other node, and further decomposition is carried out if and only if it renders the number of coefficients required for an adequate representation

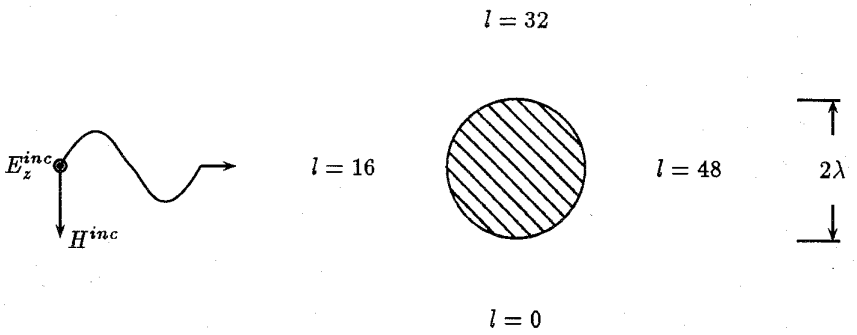


Fig. 3. Scattering problem of a circular conducting cylinder excited by a TM incident plane wave.

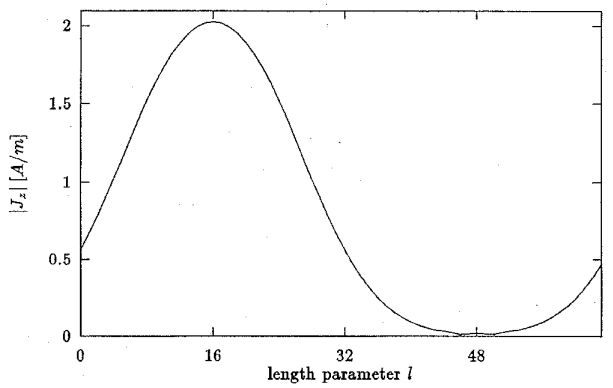


Fig. 4. Magnitude of current density $J_z$ along the circular perimeter of the scatterer for the scattering problem illustrated in Fig. 3.

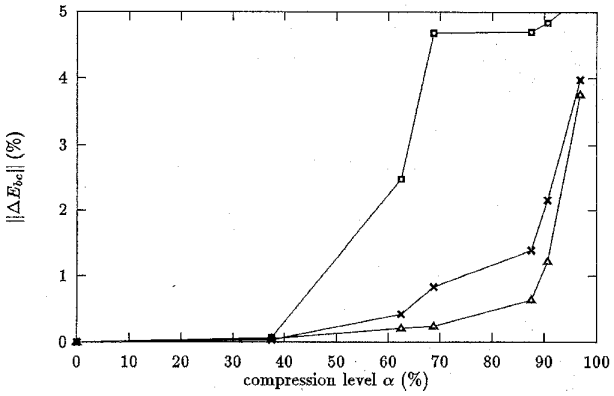


Fig. 5. Boundary condition error versus compression level of the impedance matrix for the scattering problem illustrated in Fig. 3. Cases considered are for wavelet transform basis functions (△) windowed Fourier transform basis function (□) and adaptively constructed basis functions (×).

of the signal smaller. This procedure can be classified as "top-down near-best basis algorithm, with an additive cost function" (see [14], for example). The cost function we employ in this paper is given by

$$\mathcal{C}(\vec{x}) \triangleq - \sum_{i:\, x_i \neq 0} x_i^2 \ln x_i^2, \quad \vec{x} = \{x_i\} \tag{9}$$

where $\vec{x}$ is a vector whose elements are the signal coefficients related to the node under consideration. Note that there are two such vectors associated with each node, corresponding respectively to the signal coefficients before and after the decomposition. The length of $\vec{x}$ is $N/2^r$, where $N$ is the length of the input signal and $r$ $0 \leq r < \log_2(N)$ is an integer designating the number of decomposition stages the signal goes through until it reaches the node. Once the desired tree structure has been determined, which means that a basis has been selected, we apply the same transformation to $[Z]$, to the sources, and to the excitation vector $\vec{V}$ to obtain a transformed system. However, instead of thresholding the impedance matrix in a conventional manner, it is compressed to a reduced-size form. This is effected by singling out a small number of basis functions which correspond to large values in the decomposition of $\vec{V}$. It is then assumed that these basis functions are sufficient to accurately represent the unknown and, hence, we keep only the matrix elements needed for finding out the coefficients of these basis functions. The result is a reduced-size matrix equation which is by far easier to solve. Its solution gives the coefficients of the dominant terms in the series expansion of the current. The dominant terms are expected to approximate the true current close enough for all practical purposes.

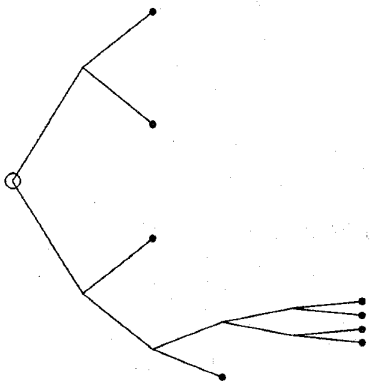

Fig. 6. Tree structure representation for the basis functions adaptively constructed for the scattering problem illustrated in Fig. 3.

To measure the reduction in the size of the impedance matrix, we define a scalar quantity $\alpha$, which is referred to hereafter as the compression level. The compression level is defined as the ratio between the number of elements omitted, while casting the impedance matrix into the compressed form

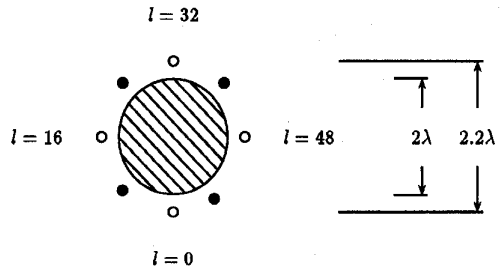


Fig. 7. Scattering problem of a circular-conducting cylinder, excited by a surrounding array of filamentary sources.

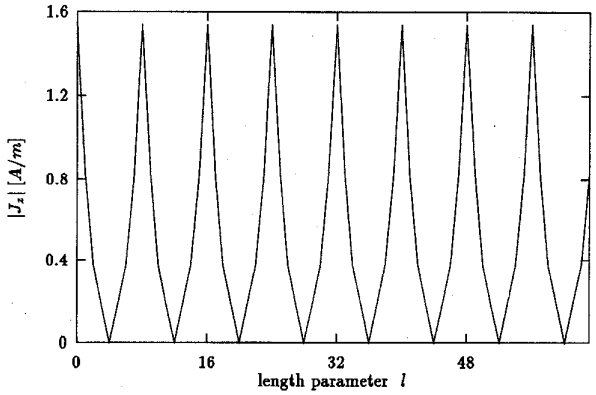


Fig. 8. Magnitude of current density $J_z$ along the circular perimeter of the scatterer for the scattering problem illustrated in Fig. 7.

and the number of elements in the original matrix. To describe the compression level mathematically, assume that the size of the original matrix is $N \times N$ and that the size of the reduced matrix is $M \times M$. Then, the relation between $\alpha$ and $M$ is given by

$$\alpha = \frac{N^2 - M^2}{N^2} \tag{10}$$

or written alternatively as

$$M = N\sqrt{1-\alpha}. \tag{11}$$

Note that in the above method, the prevailing assumption is that there is a resemblance between the modified excitation vector $\vec{V}$, which reflects both the geometry of the scatterer and the excitation and the resultant solution vector. One may argue that instead of using $\vec{V}$, we could have used the approximate physical optics current. This might have been preferable, but would definitely require much more computations than those needed for just modifying $\vec{V}$. It should be also added that the inherent dependence of the method on the excitation vector implies that with each change in the excitation one may have to follow the basis selection procedure from the start. Hence, when a problem ought to be solved for various excitations, as in the case of RCS computations, the method might be somewhat less attractive.

## VI. Numerical Example

In this section, we present four numerical examples. In the first three examples the same scatterer is considered for various

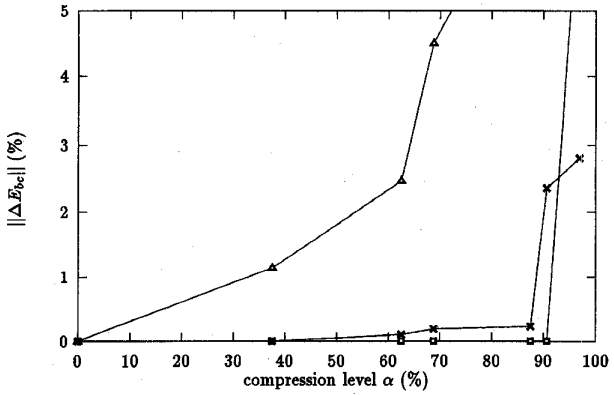


Fig. 9. Boundary condition error versus compression level of the impedance matrix for the scattering problem illustrated in Fig. 7. Cases considered are for wavelet transform basis functions (△), windowed Fourier transform basis functions (⊟) and adaptively constructed basis functions (×).

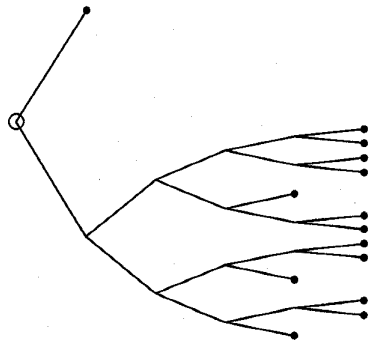

Fig. 10. Tree structure representation for the basis functions adaptively constructed for the scattering problem illustrated in Fig. 7.

excitations and, hence, the basis functions constructed in each case are different. In the fourth example, a different scatterer is considered for the same excitation taken in the first example.

The purpose of presenting these examples is threefold. First, we demonstrate that the adaptively-constructed basis functions can excel both the commonly used wavelet transform basis functions as well as the windowed Fourier transform basis functions. Second, we show that the resulting basis functions conform to both the geometry of the scatterer and the excitation. Finally, we make a point that by using the above described method of matrix compression, one gains an insight into the basis selection process. This suggests that by inspecting the geometry of the scatterer and the excitation one can foresee whether the adaptively-constructed basis functions are going to be more or less like one of the above mentioned two bases, or better than both of them.

In the first three examples, we consider scattering by a perfectly conducting cylinder of circular cross section. The current over the cylinder is expanded in terms of 64 equally spaced pulse basis functions, and we use twice this number of equally spaced pulse functions for testing. The maximum depth of the tree structure of digital filters is taken to be five. This is equivalent to letting the longest basis function be made up of $2^5 = 32$ pulse functions. Thus, it follows that a) all

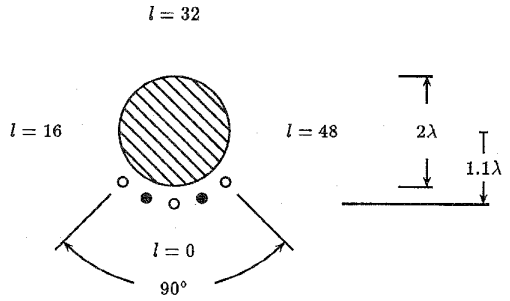


Fig. 11. Scattering problem of a circular-conducting cylinder, excited by a partially surrounding array of filamentary sources.

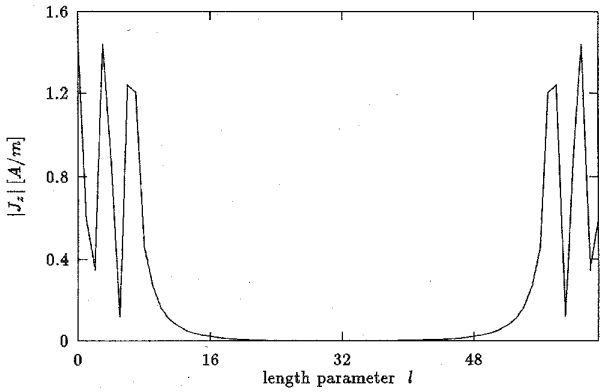


Fig. 12. Magnitude of current density $J_z$ along the circular perimeter of the scatterer for the scattering problem illustrated in Fig. 11.

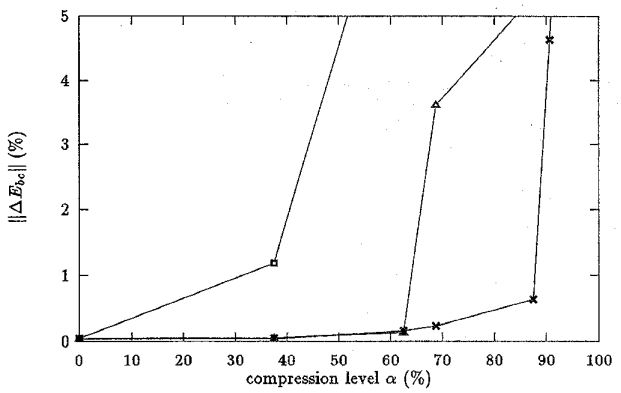


Fig. 13. Boundary condition error versus compression level of the impedance matrix for the scattering problem illustrated in Fig. 11. Cases considered are for wavelet transform basis functions (△) windowed Fourier transform basis functions (□) and adaptively constructed basis functions (×)

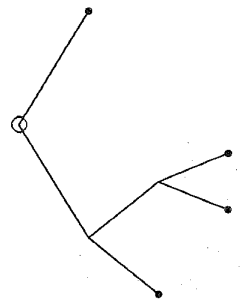

Fig. 14. Tree structure representation for the basis functions adaptively constructed for the scattering problem illustrated in Fig. 11.

the windowed Fourier transform basis functions will consist of 32 pulse functions, b) among the wavelet transform basis functions two and only two basis functions will consist of 32 elements, and c) the longest basis functions picked by the adaptive basis selection process can be of length 32 but they might as well be shorter.

In the first example, described in Fig. 3, the excitation is a TM plane wave of unit-amplitude magnetic field. The resulting current is shown in Fig. 4. The three cases, namely using wavelet transform, using windowed Fourier transform, and that of using adaptively constructed basis functions, are compared with each other in Fig. 5. This figure shows a plot of the boundary condition error as a function of the compression level. The boundary condition error is defined as the average square error on the scatterer surface normalized to the average square incident field on the scatterer surface. The compression level has been defined in Section V. Observing Fig. 5, it can be readily noted that when no compression of the matrix is taking place, the three cases yield *exactly* the same result. However, when compression is applied the difference in performance is evident. In this case, the wavelet transform basis functions are better suited for the configuration than the windowed Fourier transform basis functions. It is seen that the adaptively constructed basis functions yield results similar to those obtained with wavelet transform basis functions. In Fig. 6, the tree structure picked in the adaptive basis selection process is shown. This tree structure is neither that of wavelets nor that of the windowed Fourier transform, though it more closely resembles the wavelet tree structure. Hence, the results are very similar, yet not identical, to those of the basis functions of a wavelet transform tree structure of depth five.

In the second example, the same scatterer is considered, but this time the excitation is due to eight adjacent current filaments of 377 [mA] amplitude and alternating polarity, arranged as illustrated in Fig. 7. The resulting current on the scatterer is depicted in Fig. 8. The three cases, namely using wavelet transform, using windowed Fourier transform, and that of using adaptively constructed basis functions, are compared with each other in Fig. 9. In this case, the windowed Fourier transform basis functions yield better results than the wavelet transform basis functions. This is to be anticipated in view of the fact the current is periodic and, thus, can be effectively expanded in terms of windowed Fourier transform basis functions. Again, the performance of the adaptively constructed basis functions is as expected very similar to that of the windowed Fourier transform basis functions. The tree structure resulting from this adaptive basis selection process is shown in Fig. 10 and, indeed, this structure is similar to the windowed Fourier transform tree structure. Also note that it is completely different from the previously chosen tree shown in Fig. 6.

The third example considered is for the excitation depicted in Fig. 11, where again the amplitude of each of the filaments

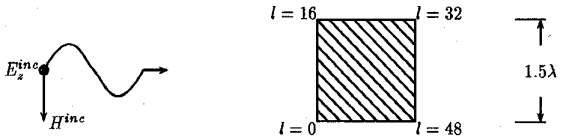


Fig. 15. Scattering problem of a conducting cylinder of square cross section excited by a TM incident plane wave.

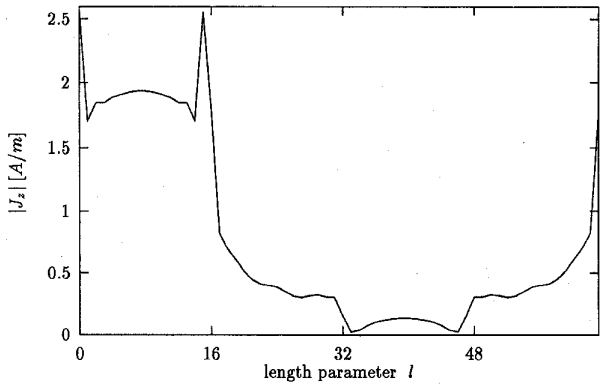


Fig. 16. Magnitude of current density $J_z$ along the perimeter of the scatterer for the scattering problem illustrated in Fig. 15.

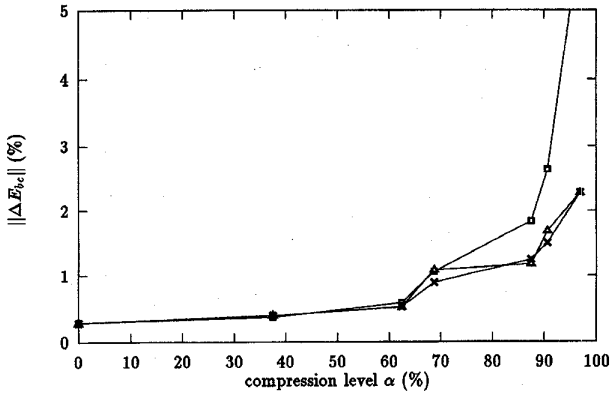


Fig. 17. Boundary condition error versus compression level of the impedance matrix for the scattering problem illustrated in Fig. 15. Cases considered are for wavelet transform basis function (△) windowed Fourier transform basis functions (⊟) and adaptively constructed basis functions (×)

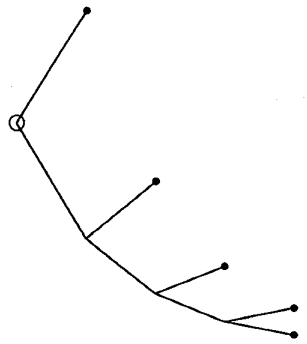

Fig. 18 Tree structure representation for the basis functions adaptively constructed for the scattering problem illustrated in Fig. 15.

is 377 [mA], and the filaments are with alternating polarity. A plot of the resulting current on the scatterer is shown in Fig. 12. This current is periodic only over part of the scatterer boundary surface. A plot of the performance achieved with the various basis functions is given in Fig. 13. In this case, it is clearly seen that the adaptively constructed basis functions are preferable over the two other bases. The tree structure for the adaptively constructed basis functions is shown in Fig. 14 and appears to consist of two levels only. Thus, it is neither similar to the wavelet transform tree nor to the windowed Fourier transform tree, and it evidently yields better results.

The last example is perhaps the most convincing one, as the adaptation process yields basis functions which are clearly related to our physical understanding of the problem. In the last example, we consider a square cylinder illuminated by a TM plane wave, as described in Fig. 15 (again, the plain wave is of unit-amplitude magnetic field). A plot of the current induced on the scatterer surface is shown in Fig. 16. A plot of the performance achieved with the various basis functions is given in Fig. 17. The results obtained using the adaptively-constructed basis functions are quite similar to those obtained using the wavelet transform basis functions. This can also be seen from the tree structure shown in Fig. 18, picked by the adaptive basis selection process. This tree structure is a wavelet transform tree structure of depth four. Thus, the longest basis function is made up of $2^4 = 16$ pulse functions which is exactly the number of pulse functions needed for covering each side of the rectangular.

More understanding of the process can be gained from Fig. 19 where the resulting current, under certain compression terms of the matrix, is shown for the adaptively constructed basis functions and for the windowed Fourier transform basis functions. The fact that the latter are, in essence, global basis functions is evident from the fact that the changes introduced with each additional term are felt everywhere. This is in contrast to the current obtained for the adaptively constructed basis functions which are not necessarily long and, hence, the changes introduced with each additional term are localized.

## VII. Summary and Conclusion

In this paper, we have described a new method for the incorporation of the wavelet transform into existing numerical solvers. This incorporation involves the use of digital filters to obtain transformation of the regular pulse-based impedance matrix. The idea of wave packets has been presented to demonstrate the flexibility in the choice of basis functions offered by the new approach; its application to a scattering problem has been shown to yield better results than those obtained using regular wavelets. Many of the ideas presented still need further furnishing, such as the possibility of choosing different filters type, better approximation of the current (not merely by using the modified excitation vector), and others. It is believed that in an analogous way, other techniques based on the theory of digital filters can be put into use for solving electromagnetic scattering problems.

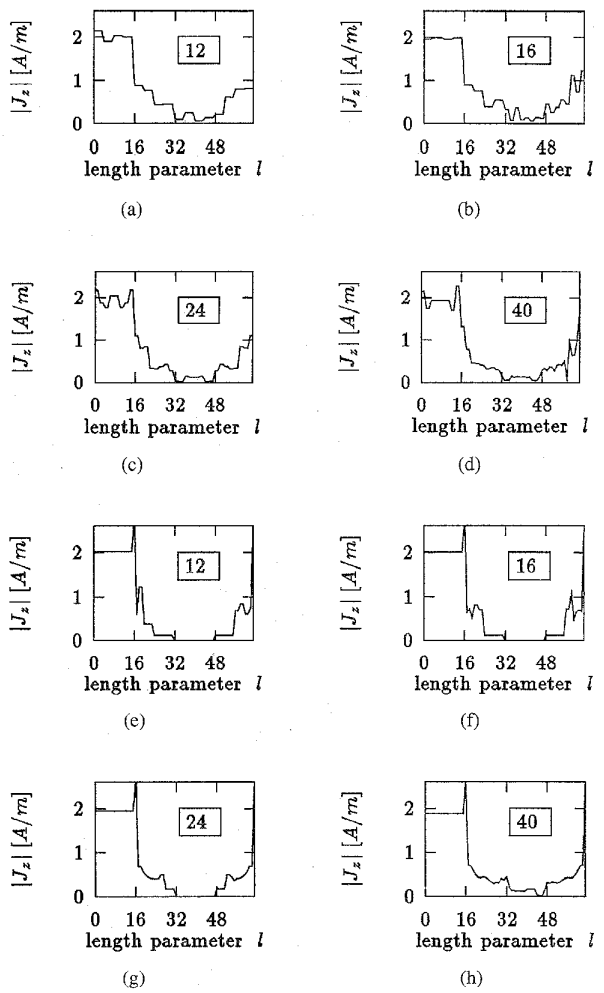


Fig. 19. Magnitude of current density $J_z$ along the square perimeter of the scatterer obtained by taking partial sums from the 64-term series expansion. Cases considered are for (a)–(d) windowed Fourier transform basis functions and (e)–(h) adaptively constructed basis functions. The number of dominant terms is indicated in each figure in a box.

## REFERENCES

[1] B. Z. Steinberg and Y. Leviatan, "On the use of wavelet expansions in the method of moments," *IEEE Trans. Antennas Propagat.*, vol. 41, pp. 610–619, May 1993.

[2] O. P. Franza, R. L. Wagner, and W. C. Chew, "Wavelet-like basis functions for solving scattering integral equations," in *IEEE AP-S Int. Symp. Dig.*, 1994, vol. 1, pp. 3–6.

[3] Y. Leviatan, Z. Baharav, and E. Heyman, "Analaysis of electromagnetic scattering using arrays of fictitious sources," *IEEE Trans. Antennas Propagat.*, vol. 43, pp. 1091–1098, Oct. 1995.

[4] F. X. Canning, "Improved impedance matrix localization method," *IEEE Trans. Antennas Propagat.*, vol. 41, pp. 659–667, May 1993.

[5] ———, "The impedance matrix localization (IML) method for moment-method calculations," *IEEE Antennas Propagat. Soc. Mag.*, vol. 32, no. 5, pp. 18–30, Oct. 1990.

[6] R. L. Wagner, G. P. Otto, and W. C. Chew, "Fast waveguide mode computation using wavelet-like basis functions," *IEEE Microwave Guide Wave Lett.*, vol. 3, pp. 208–210, July 1993.

[7] M. Vetterli and C. Herely, "Wavelets and filter banks: Theory and design," *IEEE Trans. Acoust., Speech, Signal Processing*, vol. 40, pp. 2207–2232, Sept. 1992.

[8] W. H. Press, S. A. Teukolsky, W. T. Vetterling, and B. P. Flannery, *Numerical Recepies in C.* Cambridge: Cambridge Univ. Press, 1988, ch. 13.10.

[9] C. Taswell and K. C. McGill, "Algorithm 735: Wavelet transform algorithms for finite-duration discrete-time signals," *ACM Trans. Mathematic. Software*, vol. 20, no. 3, pp. 398–412, Sept. 1994.

[10] O. Rioul, "Fast algorithms for discrete and continuous wavelet transforms," *IEEE Trans. Inform. Theory*, vol. 38, pp. 569–586, Mar. 1992.

[11] R. R. Coifman and M. V. Wickerhauser, "Entropy-based algorithms for best basis selection," *IEEE Trans. Inform. Theory*, vol. 38, pp. 713–718, Mar. 1992.

[12] R. R. Coifman, Y. Meyer, and V. Wickerhauser, "Size properties of wavelet pakets," in *Wavelets and Their Application*, M. B. Ruskai, Ed. MA: Jones Bartlet Publ., 1992, pp. 453–470.

[13] C. Taswell, "Top-down and bottom-up tree search for selecting bases in wavelet packet transforms," in *Wavelets and Statistics*, A. Antoniadis and G. Oppenheim, Eds. New York: Springer Verlag, 1995, lecture notes in statistics.

**Zachi Baharav** received the B.Sc. degree from Tel-Aviv University, Israel, and the M.Sc. degree from the Technion-Israel Institute of Technology, Haifa, in 1986 and 1994, respectively, both in electrical engineering. He is currently working toward the Ph.D. degree in electrical engineering at the Technion-Israel Institute of Technology.

His interests are in numerical methods in electromagnetics and fractal image compression.

**Yehuda Leviatan** (S'81–M'86–SM'88) received the Ph.D. degree in electrical engineering from Syracuse University, NY, in 1982.

During 1982, he spent a year as an Assistant Professor at Syracuse University, NY. Since October 1983, he has been on the Faculty of the Department of Electrical Engineering at the Technion-Israel Institute of Technology, Haifa, where he is presently an Associate Professor. His research interest is primarily in computational electromagnetics, and his recent work deals with the use of wavelet expansions in the method of moments.